THEORETICA CHIMICA ACTA

Theoret. Chim. Acta (Berl.) 65, 167–177 (1984)

Electronic structure, geometry, and energetics of carbanion and carbocation of [1.1]ferrocenophane: An INDO study

A. Waleh*, M. L. Cher and G. H. Loew

Molecular Theory Laboratory, The Rockefeller University, 701 Welch Road, Suite 203, Palo Alto, CA 94304, USA

U. T. Mueller-Westerhoff

Department of Chemistry, University of Connecticut, Storrs, CT 06268, USA

INDO-SCF calculations with constrained geometry optimization have been performed to determine the bridge geometries in [1.1]ferrocenophane and its carbocation and carbanion to address the question of possible C—H—C hydrogen bonding in the carbanion derivative. In the equilibrium geometry of the carbanion, the endo-hydrogen is bonded to one of the bridge carbon atoms and the calculated distance between the two bridge carbons seems too large to accommodate a stable C—H—C hydrogen bond. The results indicate that the observed proton NMR spectrum of carbanion should be interpreted in terms of rapid proton exchange between two bridge carbon atoms rather than a symmetric hydrogen bond. The ground state charge distributions show that the ionic bridges in both carbanion and carbocation are highly conjugated and most of the ionic charge in both molecules is distributed over the ferrocene ring system. The charge on the iron varies only slightly among the three molecules and the formal oxidation state of iron remains +2. The role of the iron seems to be that of a conduit for charge transfer between ferrocene rings upon conjugation.

Key words: INDO—[1.1]ferrocenophane—carbanion of—carbocation of—hydrogen bonding

* To whom all correspondence should be addressed

1. Introduction

Recent successes in the synthetic routes to produce [1.1]ferrocenophane in high yields [1–3] have been crucial in preparing large quantities of this compound and several of its important derivatives for experimental studies [3–5]. The importance of [1.1]ferrocenophane stems from its ability to produce hydrogen when it is dissolved in strong aqueous acidic media [6], resulting in a stable dication which can be reduced quantitatively to the neutral species. Thus, as a potential catalyst for the photochemical splitting of water, it is an interesting candidate for the modification of semiconductor surfaces [7, 8] in solar energy systems. NMR studies of [1.1]ferrocenophane [3] show that the molecule undergoes a rapid syn-syn exchange which occurs at a faster rate than the NMR time scale due to its small activation barrier. It is apparent that the exceptional ability of this molecule to undergo rapid conformational change and to accommodate charge relaxations, mediated by the metal centers, is crucial to its function and properties.

Removal of a proton or a hydride ion from one of the two methylene bridges linking the ferrocene units of [1.1]ferrocenophane results in the formation of a stable carbanion [5] or carbocation [4], respectively. NMR spectra [4, 5] show that both derivatives are rigidly fixed in the syn conformation in contrast to the parent compound. The NMR studies of the carbanion of [1.1]ferrocenophane and its methyl substituted derivatives [5] have posed the interesting problem of rapid proton transfer between two carbon atoms of the bridges which was interpreted as evidence for an intramolecular C—H—C hydrogen bond in this molecule [5]. Whether the intramolecular hydrogen bonding is symmetric, single-well, or corresponds to a double-well potential with a small exchange barrier has not been resolved. The NMR spectrum shows no observable temperature dependence from +30° to −70°C [5].

It appears that, for both carbanion and carbocation derivatives, the bridge orientations relative to the cyclopentadienyl planes and the degree of conjugation across the bridging carbons as well as the degree of hybridization of these carbon atoms play significant roles in their properties. Comparison of the crystal structure of the carbocation [4, 9] with that of the 1,12-dimethyl[1.1]ferrocenophane [10, 11] shows that the carbonium carbon is drawn towards the center of the cation which may account for the stabilization effects in this molecule. The existence of a C—H—C hydrogen bond in the carbanion should also be critically dependent on the distance between the bridging carbons and on the hybridization of these atoms [5]. The equilibrium geometry of the carbanion, however, has not been determined.

In previous work [12], it was shown that the application of a semiempirical Intermediate Neglect of Differential Overlap (INDO-SCF-CI) method with spectroscopic parameterization, capable of handling transition metals [12, 13], provides reasonable description of ferrocene and ferrocenium ion systems in agreement with the observed photoelectric and electronic spectra and the results of *ab initio* calculations. In particular, the ground-state charge distributions

and the charge relaxations upon ionization are accurately predicted. The method also has the capability of calculating equilibrium geometries by a gradient technique with the appropriate parameters for energy calculations. The theoretically obtained optimized geometries can then be used as input to the program with spectroscopic parameterization in order to obtain electronic structure information. For ferrocenophane systems, this procedure should prove very useful, since much of the dynamic behavior of these molecules may not, in any event, be easily determined from the equilibrium crystal molecular structures.

In the present communication we describe the application and limitations of the geometry optimization calculations for ferrocenophane systems and show that, under appropriately constrained conditions, the bridge geometries can be correctly determined. The method is then used to characterize the ground state geometry and the electronic structure of carbanion of [1.1]ferrocenophane. The main objective of the paper is to address the question of an intramolecular symmetric C—H—C hydrogen bond versus a rapid proton transfer exchange between two equivalent positions on the carbanion. A separate discussion relevant to the mechanisms of protonation and hydrogen liberation for [1.1]ferrocenophane in aqueous acidic media is presented elsewhere [14].

2. Method

A detailed description of the INDO-SCF method has been given previously [12, 13]. Spectroscopic parameterization where the two-electron repulsion integrals are evaluated from an empirical Weiss–Mataga–Nishimoto formula [12, 15, 16] is ideally suitable for the calculation of ground-state electronic structure and properties of transition-metal complexes from an equilibrium geometry. Geometry calculations were carried out with the appropriate options in the method where the two-electron repulsion integrals are calculated theoretically and the resonance integrals are set to values suitable for energy calculations. The optimized geometries are obtained from a gradient technique in the cartesian coordinate system.

In preliminary calculations of the known geometries of ferrocene [17, 18] and ferrocenophane systems [4, 9–11], it was determined that the optimized final geometries were similar to the observed geometries with the exception of the ring-metal distances which, at about 1.87 Å, were considerably larger than the experimental value of 1.65 Å. In particular, the orientation of the bridge carbons relative to the cyclopentadienyl rings in ferrocenophane systems were correctly calculated. It should be noted that *ab initio* calculations of ferrocene equilibrium geometry, with both minimal and double-zeta basis sets [19], also predict a similar ring-metal distance of 1.9 Å. However, potential energy calculations of metallocenes with an all-electron-SCF-multiple scattering $X\alpha$ method [20] have produced equilibrium ring-metal distances in agreement with the experimental values. We suspect that the longer calculated ring-metal distances in sandwich compounds by the present INDO method are the consequence of the *d*-orbital exponents which, otherwise, produce reasonable transition metal bond distances.

Ring-ring separation will sensitively affect the charge relaxation and conjugation in ferrocenophane systems. Also, any possible C—H—C hydrogen bonding would critically depend on the bridge carbon distances. Accordingly, all subsequent calculations were carried out with the additional constraints of holding the z-components of the ring carbon atoms fixed in a cartesian coordinate system in which the y-axis coincides with the axis of C_2 symmetry of the molecule and the iron atoms are positioned on the x-axis. Since the main objective is the determination of the bridge geometries, these constraints will not severely affect the results. Two degrees of freedom for each ring carbon and all degrees of freedom for all other atoms remain unconstrained. In particular, since the bridge carbons and the iron atoms are totally free of constraint, limited relaxation in the ring orientations and ring-metal distances are allowed. The above set of constraints is equivalent to a systematic energy increase of about 100 kcal/mole from that of a totally relaxed geometry.

3. Results

The geometry optimization calculations were first carried out for the case of the carbocation of [1.1]ferrocenophane with the crystal molecular structure [4, 9] as input. The calculations were repeated using several severe deformations of the

Table 1. Comparison of the optimized geometries of [1.1]ferrocenophane and its carbocation with the observed crystal structure data

	Carbocation		Neutral	
	Obs.[a]	Calc.	Obs.[b]	Calc.
Fe···Fe	4.66	4.52	4.62	4.62
Fe···C_{ring}[c]	2.05	2.05	2.03	2.10
$(C—C)_{ring}$[c]	1.45	1.44	1.41	1.43
Methylene Bridge[d]:				
Fe—C_1[c]	3.26	3.23	3.22	3.23
$C_2—C_1$	1.51	1.46	1.49	1.46
$C_{22}—C_1$	1.52	1.46	1.52	1.46
$<(C_2—C_1—C_{22})$	119.0°	122.8°	117.6°	120.2°
$<(C—C_1—H)$[c]		107.3°		108.1°
$<(H_A—C_1—H_B)$		102.8°		102.6°
Ionic Bridge[d]:				
Fe—C_{12}[c]	2.98	2.99	3.23	3.23
$C_{11}—C_{12}$	1.39	1.39	1.49	1.46
$C_{13}—C_{12}$	1.44	1.39	1.52	1.46
$<(C_{11}—C_{12}—C_{13})$	123.2°	132.3°	117.6°	120.2°
$<(C—C_{12}—H)$[c]		113.9°		
Bridge Carbons Distance[d]:				
$C_1—C_{12}$	3.52	3.72	3.68	3.73

[a] Refs. [4] and [9].
[b] Refs. [10] and [11].
[c] Average values.
[d] Numbering is the same as in Ref. [11] and Figs. 1 and 2.

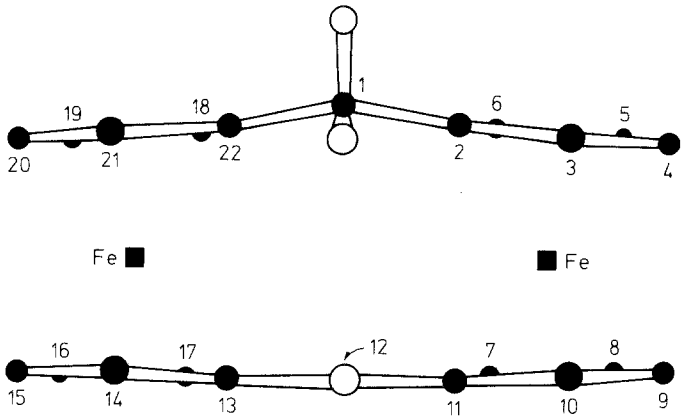

Fig. 1. Side view (*xz*-plane projection) of the optimized geometry of the carbocation of [1.1]ferrocenophane. Symbols: ■, Fe; ●, Carbon; ○, Hydrogen

bridge atoms as initial geometries. In all cases, optimization yielded the same final geometry which was, moreover, similar to the observed structure of the carbocation. Table 1 shows a comparison of the calculated and observed values of the important intramolecular distances and bond angles. A side view (*xz*-plane projection) of the molecule is also given in Fig. 1. The secondary carbon of the methylene bridge is 0.29 Å above the average horizontal plane through the tertiary carbons as compared to the observed value 0.22 Å. By contrast, the calculated positions of the carbonium ion center and its attached hydrogen atom are roughly in the same horizontal plane with its neighboring tertiary carbons. The carbonium ion center is about 0.16 Å above this plane towards the center of the cation in the crystal. The planar geometry of the ionic bridge is connected to the charge conjugation across the carbonium ion center. The calculated charge distributions obtained from spectroscopic parameters for the optimized equilibrium geometry of the carbocation is shown in Table 2.

Similar calculations were carried out for the neutral [1.1]ferrocenophane. A comparison of the calculated and the observed values [10, 11] of the important geometrical data is also given in Table 1. All values are in reasonable agreement. The slightly longer calculated distance between the iron and ring carbon atoms is due to the large dihedral angle between the two cyclopentadienyl rings in the starting geometry [11]. This gives rise to small components of the ring-ring normal distance along the *x*- and *y*-coordinates which are constraint-free in these calculations. The deviation corresponds to an angle of twist of about 29 degrees for the cyclopentadienyl rings of the ferrocene units as compared to the observed value [11] of 21.5 degrees. Full optimization calculations with no constraint, however, result in the same angle of twist as observed in the crystal but at a longer ring-ring distance of about 3.75 Å. The calculated charge distributions with spectroscopic parameters for the crystal and optimized molecular geometries of [1.1]ferrocenophane, as presented in Table 2, show that the ring carbon charges and the relaxation effects are sensitively affected by ring separation and twisting.

Table 2. Ground-state Mulliken charge distributions in carbocation, neutral, and carbanion species of [1.1]ferrocenophane

Atoms[a]	Carbocation calc. geom.	Neutral X-tal[b] geom.	Neutral calc. geom.	Carbocation-like calc. geom.	Carbanion Neutral-like calc. geom.	Carbanion Neutral-like X-tal[b,c] geom.
Fe	2.003	2.056	1.670	1.953	1.630	2.033
α-Carbons:						
C_6	−0.279	−0.249	−0.207	−0.287	−0.200	−0.251
C_7	−0.252	−0.257	−0.305	−0.315	−0.331	−0.273
C_{17}	−0.266	−0.249	−0.207	−0.328	−0.247	−0.267
C_{18}	−0.271	−0.257	−0.305	−0.274	−0.316	−0.273
α'-Carbons:						
C_3	−0.262	−0.279	−0.299	−0.283	−0.313	−0.294
C_{10}	−0.250	−0.273	−0.196	−0.311	−0.225	−0.289
C_{14}	−0.245	−0.279	−0.299	−0.304	−0.330	−0.304
C_{21}	−0.276	−0.273	−0.196	−0.301	−0.200	−0.281
β-Carbons:						
C_5	−0.231	−0.287	−0.197	−0.280	−0.214	−0.309
C_8	−0.196	−0.266	−0.249	−0.281	−0.284	−0.287
C_{16}	−0.208	−0.287	−0.197	−0.293	−0.224	−0.307
C_{19}	−0.229	−0.266	−0.249	−0.275	−0.274	−0.287
β'-Carbons:						
C_4	−0.219	−0.271	−0.243	−0.273	−0.265	−0.294
C_9	−0.200	−0.289	−0.184	−0.276	−0.207	−0.310
C_{15}	−0.197	−0.271	−0.243	−0.272	−0.280	−0.294
C_{20}	−0.226	−0.289	−0.184	−0.281	−0.210	−0.311
Ring Hydrogens:						
H[d]	+0.084	+0.055	+0.060	+0.038	+0.039	+0.035
Tertiary Carbons:						
C_2	−0.168	−0.160	−0.150	−0.169	−0.138	−0.156
C_{11}	−0.187	−0.176	−0.153	−0.109	−0.085	−0.134
C_{13}	−0.192	−0.160	−0.150	−0.109	−0.084	−0.107
C_{22}	−0.176	−0.176	−0.153	−0.174	−0.139	−0.173
Methylene Bridge:						
C_1	−0.063	−0.088	−0.061	−0.061	−0.058	−0.086
H(EXO)	+0.075	+0.053	+0.050	+0.022	+0.026	+0.028
H(ENDO)	+0.046	+0.049	+0.043	+0.047	+0.054	+0.062
Ionic Bridge:						
C_{12}	+0.024			−0.317	−0.319	−0.426
H	+0.097			−0.014	−0.013	+0.003

[a] Numbering is the same as in Ref. [11] and Figs. 1 and 2.
[b] Ref. [11].
[c] Coordinates of the anionic bridge hydrogen are modified.
[d] Average values.

The bridge geometries in neutral [1.1]ferrocenophane are sharply different from those in the carbocation. The secondary carbons of both bridges are 0.22 Å above and below the average horizontal planes through their corresponding tertiary

Table 3. Calculated optimized bridge geometries for carbanion of [1.1]ferrocenophane

	Carbocation-like input geometry	Neutral-like input geometry
Methylene Bridge[a]:		
$Fe-C_1$[b]	3.24	3.24
C_2-C_1	1.46	1.46
$C_{22}-C_1$	1.46	1.46
$<(C_2-C_1-C_{22})$	125.3°	121.8°
$<(C-C_1-H)$[b]	106.8°	107.7°
$<(H_A-C_1-H_B)$	102.2°	102.5°
Anionic Bridge[a]:		
$Fe-C_{12}$[b]	3.23	3.22
$C_{11}-C_{12}$	1.40	1.41
$C_{13}-C_{12}$	1.40	1.40
$<(C_{11}-C_{12}-C_{13})$	125.0°	125.3°
$<(C-C_{12}-H)$[b]	116.0°	116.0°
Bridge Carbon Distance[a]:		
C_1-C_{12}	3.91	3.67

[a] Numbering is the same as in Ref. [11] and Figs. 1 and 2.
[b] Average values.

carbons, respectively, away from the center of the molecule. The corresponding observed value in the crystal is 0.2 Å.

To calculate the optimized bridge geometries for the carbanion of [1.1]ferrocenophane, crystal structures of both neutral and carbocation were used as initial geometries. The resulting bridge geometries are shown in Table 3. Although the constraints of fixed ring-carbon *z*-coordinates allow little variation in the geometries of the ferrocene portions of the molecule, both initial geometries led to a similar orientation of the bridge carbons relative to the tertiary carbons. Fig. 2 shows side views (*xz*- and *yz*-plane projections) of the bridge geometries in all three molecules. In contrast to the carbonium ion of the carbocation (Fig. 2c), the carbanion bridge carbon is tilted away from the center of the molecule (Fig. 2b) to a similar position as in the neutral species (Fig. 2a). However, the hydrogen attached to the carbanion center swings inward and assumes a nearly coplanar position with the two bridge C—C bonds.

The charge distribution in the carbanion depends on the choice of geometry for the ferrocene units. Although this cannot be determined in the present calculations due to the limitations imposed by the constraints, the two calculated carbocation-like and neutral-like ferrocene geometries probably form two extremes of the possible ferrocene geometries of carbanion. In fact, due to the smallness of the activation barrier for conformational changes in [1.1]ferrocenophane, as evident from temperature-dependent NMR observations [3], it is improbable that a unique orientation of the ferrocene units can be obtained within the accuracy of semiempirical calculations. Full optimization calculations of the carbanion, without any

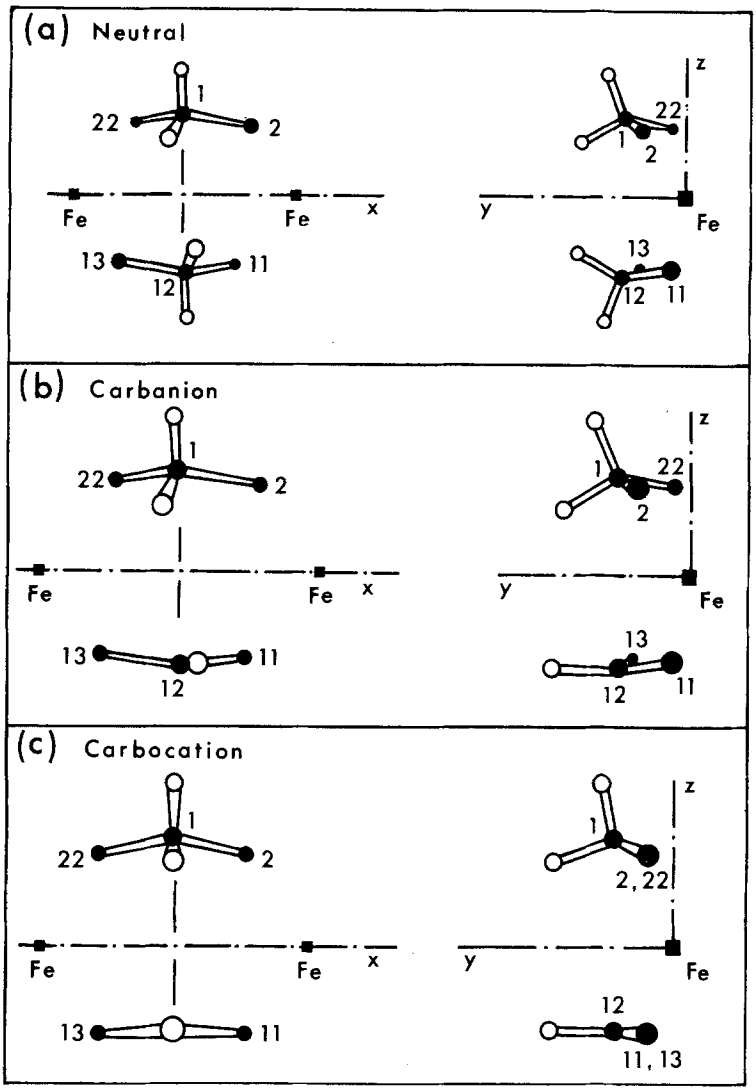

Fig. 2. Side views (*xz*- and *yz*-plane projections) of the bridge geometries in: (a) [1.1]ferrocenophane, (b) its carbanion, and (c) carbocation derivatives. Symbols: ■, Fe; ●, Carbon; ○, Hydrogen

constraint, with either carbocation- or neutral-like structure as starting geometries, preserve the ferrocene geometries with the exception of the lengthening of the ring-metal distance to 1.87 Å. The calculated energy difference between the two final conformations is less than 1 kcal/mole which implies that the ring orientations in the molecule can change at the expense of very little energy. The calculated charge distributions in the carbanion for three different ferrocene geometries are shown in Table 2. Two of the geometries correspond to the optimized carbocation-like and neutral-like structures. Since the larger twist angle for the optimized neutral-like structure may have its origin in the constraints

used in these calculations, and since the bridge geometry of the carbanion and the neutral species are similar, charge distributions were also calculated for the corresponding crystal molecular geometry with the appropriate modification of the coordinates of the hydrogen attached to the anionic bridge carbon.

4. Discussion

From the results displayed in Fig. 2 and Table 3 it can be seen that the equilibrium geometry in the carbanion corresponds to the endo-hydrogen atom being bonded to one or the other bridge carbon atoms, i.e., to a double-well potential for proton transfer, although the calculated distance of 3.7–3.9 Å between the bridge carbons seems too large to accommodate a stable C—H—C hydrogen bond in this molecule. The proton NMR spectrum of the carbanion (doublet at 3.09 ppm and triplet at 4.51 ppm) [5] which can be thought to arise from either a rapid proton exchange or a symmetric C—H—C hydrogen bond, should on the basis of these results, be interpreted in the former way. The calculated energy barrier for this transfer process, obtained by geometry optimization with the additional constraint of confining one of the bridge hydrogens to the *xy*-plane of the iron atoms, is about 20 kcal/mole. The final geometry of this state corresponds to the symmetric inward bending of both bridge carbons to simultaneously establish a C—H bond for each of them of about 1.4 Å for a neutral-like ferrocene structure. This implies a transition state with a symmetric C—H—C hydrogen bond. However, the actual value of the energy barrier to H transfer should be much smaller than 20 kcal/mole, since the constraints used in these calculations do not allow for ring relaxations to compensate for the strains associated with the bending of the bridge carbon bonds. In fact, given the small energy requirement for a change in the ring orientation, we expect that the relaxation energy is considerably large.

An important aspect of the present calculations, however, is that it provides experimentally observable distinguishing features associated with either a single- or double-well potential. Fig. 2 shows that, in the equilibrium geometry of the carbanion, the anionic carbon is essentially sp^2 hybridized. Therefore, any proton-transfer process necessarily involves a concerted motion of the *exo* hydrogens, and possibly carbon atoms, as the anionic center alternates between the two bridges. This is expected to give rise to a line broadening of the bridge proton NMR resonances at low temperatures for a proton-transfer process. By contrast, the proton resonances associated with the rigid sp^3 hybridized bridge carbons in a symmetric single-well potential should remain sharp at all temperatures. Similarly, as shown in Table 2 the tertiary carbons adjacent to the anionic carbon are less negative than the ones adjacent to the methylene carbon. Therefore, the ^{13}C NMR spectrum of the tertiary carbons at low temperatures should also show line broadening in the case of a transfer process. In this regard, it is noteworthy that the high resolution ^{13}C FTNMR in the solid state, under "magic angle" spinning conditions indicates that the tertiary carbons may be inequivalent at room temperature [21]. While this result indicates the presence of a double-well potential, the inequivalence may well be due to an asymmetric location of the THF-solvated lithium counter ion.

Table 2 also shows the effect of conjugation on both the carbanion and carbocation. About 30% of the negative charge in the carbanion and only 2% of the positive charge in carbocation reside on their respective ionic bridge carbons. The rest of the charge in both molecules is distributed over the ferrocene ring system. Comparing the bridge carbon charges in carbanion, carbocation, and their neutral precursor with the ^{13}C NMR data reinforces the speculation that conjugation effects give rise to downfield shifts in the NMR spectrum [5]. Thus the similar ^{13}C NMR shift of bridge carbons of the neutral and carbanion is interpreted in terms of a near compensation of the downfield and upfield shifts due to conjugation and increased negative charge in the latter, respectively. By contrast, the extreme downfield shift of the cationic carbon at 162 ppm [4] results from the additive effect of conjugation and increased positive charge relative to the neutral molecule.

Although the observed proton NMR of the ring protons may not be directly proportional to the neighboring carbon charges due to complicated solvent effects, their comparison with the calculated ring-carbon charges may be instructive in determining the geometry of the ferrocene units in the carbanion. The changes in the calculated ring-carbon charges of the carbocation compared to those of the neutral species with crystal molecular structure (Table 2, Cols. 1 and 2) are in agreement with the observed NMR downfield shifts of the ferrocene protons of the carbocation (3.8–6.0 ppm) [4] from those of neutral ferrocenophane (4.02, 4.22 ppm) [3]. The calculated charges of the neutral species with crystal geometry are in better agreement with the spread of the ring proton NMR resonances [3] than those with the optimized geometry. The calculated ring-carbon charges with either carbocation-like or neutral-like ferrocene geometry for carbanion (Table 2, Cols. 4 and 5) are compatible with the observed four-proton multiplets at 3.6 and 4.3 ppm and an eight-proton multiplet at 3.4 ppm [5], although the neutral-like geometry is slightly favored. Since the ferrocene portion of carbocation geometry is close to having both a vertical and a horizontal plane of symmetry [4, 9], it can be argued that carbanion, too, is either rigid, with two vertical and horizontal planes of symmetry [5], or, at least, does not undergo a complete syn-syn exchange.

Although the charges on the iron atoms are sensitive functions of the geometry of the ferrocene units, comparison of charges for similar geometries shows that not more than 10% of the negative charge resides on each of the iron atoms in the carbanion. The formal oxidation state of iron atoms in all three molecules is a +2 state. The role of the iron atoms seems to be that of a conduit for the transfer of charge between cyclopentadienyl rings.

Acknowledgment. Two of the authors (A.W. and G.H.L.) gratefully acknowledge support for this work from NSF Grant PCM7921591.

References

1. Cassens, A., Eilbracht, P., Mueller-Westerhoff, U. T., Nazzal, A., Neuenschwander, M., Proessdorf, W.: J. Organomet. Chem. **205**, C17 (1981)
2. Mueller-Westehoff, U. T., Nazzal, A., Proessdorf, W.: J. Organomet. Chem. **205**, C21 (1981)

3. Cassen, A., Eilbracht, P., Nazzal, A., Proessdorf, W., Mueller-Westerhoff, U. T.: J. Am. Chem. Soc. **103**, 6367 (1981)
4. Mueller-Westerhoff, U. T., Nazzal, A., Proessdorf, W., Mayerle, J. J., Collins, R. L.: Angew. Chem. Suppl. 1982, 686 (1982)
5. Mueller-Westerhoff, U. T., Nazzal, A., Proessdorf, W.: J. Am. Chem. Soc. **103**, 7678 (1981)
6. Bitterwolf, T. E., Ling, A. C.: J. Organomet. Chem. **57**, C15 (1973)
7. Wrighton, M. S., Palazzotto, M. C., Bocarsly, A. B., Bolts, J. M., Fischer, A. B., Nadjo, L.: J. Am. Chem. Soc. **100**, 7264 (1978)
8. Nazzal, A., Mueller-Westerhoff, U. T.: submitted for publication
9. Mayerle, J. J.: private communication
10. McKechnie, J. S., Bersted, B., Paul, I. C., Watts, W. E.: J. Organomet. Chem. **8**, P29 (1967)
11. McKechnie, J. S., Maier, C. A., Bersted, B., Paul, I. C.: J. Chem. Soc. Perkin II 1973, 138 (1973)
12. Zerner, M. C., Loew, G. H., Kirchner, R. F., Mueller-Westerhoff, U. T.: J. Am. Chem. Soc. **102**, 589 (1980)
13. Bacon, A. D., Zerner, M. C.: Theor. Chim. Acta (Berl.) **53**, 21 (1979)
14. Waleh, A., Loew, G. H., Mueller-Westerhoff, U. T.: Inorg. Chem., in press
15. Weiss, K.: unpublished
16. Mataga, N., Nishmoto, K.: Z. Phys. Chem. (Wiesbaden) **13**, 140 (1957)
17. Dunitz, J. D., Orgel, L. E., Rich, A.: Acta Cryst. **9**, 373 (1956)
18. Bohn, R. K., Haaland, A.: J. Organomet. Chem. **5**, 470 (1966)
19. Luthi, H. P., Ammeter, J., Almlof, J., Korsell, K.: Chem. Phys. Letters **69**, 540 (1980)
20. Weber, J.: J. Mol. Struc. **60**, 397 (1980)
21. Mueller-Westerhoff, U. T., Nazzal, A., Yannoni, C. S.: unpublished

Received August 7/November 22, 1983